Comparison study of supercontinuum generation by molecular alignment of N_2 and O_2

Hua Cai, Jian Wu[*], Yan Peng, and Heping Zeng[‡]

State Key Laboratory of Precision Spectroscopy, East China Normal University, Shanghai 200062, China
[*]Electronic address: jwu@phy.ecnu.edu.cn
[‡]Electronic address: hpzeng@phy.ecnu.edu.cn

Abstract: We study the supercontinuum generation through femtosecond filamentation by using the quantum wake of the prealigned diatomic molecules of O_2 and N_2, where significant ultraviolet extension of the generated supercontinuum is attributed to the additional cross-focusing effect around parallel revival of molecular alignment and the consequent self-steepening as well as space-time focusing effect. Due to the discrepancy of the polarizabilities between O_2 and N_2 molecules, the spectral ultraviolet extension of the generated supercontinuum is more noticeable in molecular O_2 than that in N_2, and an extended supercontinuum spectrum from 370 to 900 nm is observed in O_2 of 2 atm. The detailed dependence of the generated supercontinuum on the pump intensity for molecular alignment and gas pressure of O_2 and N_2 molecules are performed.

References and links

1. A. Zheltikov, "Supercontinuum generation," Appl. Phys. B **77**, 143-147 (2003).
2. J. Kasparian, M. Rodriguez, G. Méjean, J. Yu, E. Salmon, H. Wille, R. Bourayou, S. Frey, Y.-B. André, A. Mysyrowicz, R. Sauerbrey, J.-P. Wolf, and L. Wöste, "White-Light Filaments for Atmospheric Analysis," Science **301**, 61-64 (2003).
3. T. Kobayashi, T. Saito, and H. Ohtani, "Real-time spectroscopy of transition states in bacteriorhodopsin during retinal isomerization," Nature **414**, 531-534 (2001).
4. A. Baltuška and T. Kobayashi, "Adaptive shaping of two-cycle visible pulses using a flexible mirror," Appl. Phys. B **75**, 427-443 (2002).
5. S. Cussat-Blanc, A. Ivanov, D. Lupinski, and E. Freysz, "$KTiOPO_4$, $KTiOAsO_4$, and $KNbO_3$ crystals for mid-infrared femtosecond optical parametric amplifiers: analysis and comparison," Appl. Phys. B **70**, S247-S252 (2000).
6. R. L. Fork, C. V. Shank, C. Hirlimann, R. Yen, and W. J. Tomlinson, "Femtosecond white-light continuum pulses," Opt. Lett. **8**, 1-3 (1983).
7. X.-J. Fang and T. Kobayashi, "Evolution of a super-broadened spectrum in a filament generated by an ultrashort intense laser pulse in fused silica," Appl. Phys. B **77**, 167-170 (2003).
8. A. L. Gaeta, "Catastrophic collapse of ultrashort pulses", Phys. Rev. Lett. **84**, 3582-3585 (2000).
9. P. B. Corkum, C. Rolland, and T. Srinivasan-Rao, "Supercontinuum generation in gases," Phys. Rev. Lett. **57**, 2268-2271 (1986).
10. F. Théberge, W. Liu, Q. Luo, and S. L. Chin, "Ultrabroadband continuum generated in air (down to 230 nm) using ultrashort and intense laser pulses," Appl. Phys. B **80**, 221-225 (2005).
11. N. Aközbek, S.A. Trushin, A. Baltuška, W. Fuß, E. Goulielmakis, K. Kosma, F. Krausz, S. Panja, M. Uiberacker, W. E. Schmid, A. Becker, M. Scalora, and M. Bloemer, "Extending the supercontinuum spectrum down to 200nm with few-cycle pulses," New J. Phys. **8**, 177 (2006).
12. F. Rosca-Pruna and M. J. J. Vrakking, "Experimental Observation of Revival Structures in Picosecond Laser-Induced Alignment of I_2," Phys. Rev. Lett. **87**, 153902 (2001).
13. T. Kanai, S. Minemoto, and H. Sakai, "Quantum interference during high-order harmonic generation from aligned molecules," Nature **435**, 470-474 (2005).
14. J. Wu, H. Qi, and H. Zeng, "Extreme-ultraviolet frequency combs by surface-enhanced optical fields with diatomic molecules," Phys. Rev. A **77**, 053412 (2008).
15. R. A. Bartels, T.C. Weinacht, N. Wagner, M. Baertschy, C. H. Greene, M. M. Murnane, and H. C. Kapteyn, "Phase modulation of ultrashort light pulses using molecular rotational wave packets," Phys. Rev. Lett. **88**, 013903 (2001).

16. S. Varma, Y.-H. Chen, and H.M. Milchberg, "Trapping and destruction of long range high intensity optical filaments by molecular quantum wakes in air," Phys. Rev. Lett. **101**, 205001 (2008).

17. F. Calegari, C. Vozzi, S. Gasilov, E. Benedetti, G. Sansone, M. Nisoli, S. De Silvestri, and S. Stagira, "Rotational Raman effects in the wake of optical filamentation," Phys. Rev. Lett. **100**, 123006 (2008).

18. J. Wu, H. Cai, H. Zeng, and A. Couairon, "Femtosecond filamentation and pulse compression in the wake of molecular alignment," Opt. Lett. **33**, 2593-2595 (2008).

19. I. V. Fedotov, A. D. Savvin, A. B. Fedotov, and A. M. Zheltikov, "Controlled rotational Raman echo recurrences and modulation of high-intensity ultrashort laser pulses by molecular rotations in the gas phase," Opt. Lett. **32**, 1275-1277 (2007).

20. H. Cai, J. Wu, A. Couairon, and H. Zeng, "Spectral modulation of femtosecond laser pulse induced by molecular alignment revivals," Opt. Lett. **34**, 827-829 (2009).

21. V. Renard, M. Renard, S. Guérin, Y. T. Pashayan, B. Lavorel, O. Faucher, and H. R. Jauslin, "Postpulse Molecular Alignment Measured by a Weak Field Polarization Technique," Phys. Rev. Lett. **90**, 153601 (2003).

22. H. Stapelfeldt and T. Seideman, "Colloquium: Aligning molecules with strong laser pulses," Rev. Mod. Phys. **75**, 543-557 (2003).

23. A. Couairon and A. Mysyrowicz, "Femtosecond filamentation in transparent media," Phys. Rep. **441**, 47-189 (2007).

24. M. Spanner, *Field-Free Alignment and Strong Field Control of Molecular Rotors* (Canada, 2004).

25. E.T.J. Nibbering, G. Grillon, M.A. Franco, B.S. Prade, and A. Mysyrowicz, "Determination of the inertial contribution to the nonlinear refractive index of air, N_2, and O_2 by use of unfocused high-intensity femtosecond laser pulses," J. Opt. Soc. Am. B **14**, 650-660 (1997).

1. Introduction

Supercontinuum (SC) generation with ultra-broadband spectra covering the spectral range from near infrared to ultraviolet (UV) has been intensively investigated in different optical media [1], and has stimulated important applications in various fields [2-5]. The SC generation is attributed to the involved nonlinear processes [6-8] such as self-phase modulation (SPM), stimulated Raman scattering, four-wave parametric process and temporal self-steepening. The first SC generation with an ultrabroad spectrum covering the spectral range from infrared to UV was obtained in high pressure gases [9]. Significant extension of spectrum in UV was achieved by the strong interaction between the intense third harmonic and fundamental pulses [10], or self-focusing of few-cycle pulse [11]. For diatomic molecules, the relative orientation between the molecular axis and field polarization can be manipulated through impulsive rotational Raman excitation [12] by ultrashort pump pulse, which leads to periodic revivals of molecular alignment after the excitation of pump pulse. The molecular alignment has been extensively studied for high harmonic generation [13, 14], ultrashort pulse compression [15], and filaments [16-18] with additional spatiotemporal phase modulation [19, 20].

In this paper, we investigate the SC generation by femtosecond filamentation in prealigned diatomic molecules of O_2 and N_2. Due to the different polarizabilities of O_2 and N_2, there is a noticeable discrepancy of the spectral UV extension in these two molecular gases. The UV extension of the SC in the spectrum of the probe pulse is mainly attributed to the additional cross-focusing effect resulted from the molecular alignment revivals, and can be manipulated by tuning the relative delay between the pump and probe pulses. The dependences of the SC generation on the pump intensity for molecular alignment and the gas pressure are studied.

2. Experiment setup

As shown in Fig. 1, our experiments were carried out with a Ti:sapphire amplified laser system (1 kHz, 800 nm, 50 fs). Both the pump and probe pulses with orthogonal polarizations were down-collimated with two separated telescope systems to obtain a large interaction volume, which were re-combined collinearly by using a thin film polarizer (TFP). The delay between the s-polarized pump pulse and the p-polarized probe one was tuned by using a motorizing translation stage in the probe arm. The collinearly recombined pump and probe pulses were then focused by using a lens with a focal length of f=60 cm into a gas cell of 85 cm, which was filled with pure molecules of O_2 or N_2 with a maximum gas pressure of 2 atm.

At the exit of the gas cell, the spectral and spatial profiles of the probe pulse were measured simultaneously by using a photomultiplier (PMT) based spectrometer (SpectraPro 750) and charge-coupled device (CCD) after an α-BBO polarizer (extinction ratio ~ 1:10^{-6}). By using a variable attenuator in the pump arm, the pulse energy of the pump could be adjusted from 0.1 to 0.57 mJ, while the probe one was fixed to 1.5 mJ.
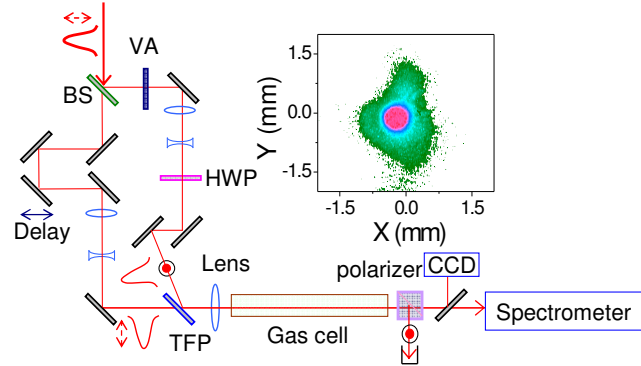

Fig. 1. The schematic of experimental setup. BS: beam splitter; VA: variable attenuator; HWP: half-wave plate; TFP: thin film polarizer; CCD: charge coupled device. The inset is the typical spatial profile of the probe pulse when the maximum UV extension of SC in parallel aligned O_2 molecules was obtained.

3. Results and discussion

Figures 2(a) and 2(c) show the measured molecular alignment revival signal of O_2 and N_2 proportional to $(<<cos^2\theta_\parallel >>-1/3)^2$ by using the weak field polarization technique [21] to reveal the polarization modulation of the probe pulse, where $\theta_\parallel$ is the angle between the molecular axis and the pump polarization. In order to do that, the polarization of the pre-attenuated probe pulse was firstly rotated by 45° and then steered to cross the pump pulse non-collinearly at a small crossing angle. The field component with polarization perpendicular to the incident probe polarization was selected by an α-BBO polarizer, which was then sent to a photodiode and analyzed by a Lock-in amplifier (SR830, Stanford). Since the pump and probe pulses were set to have orthogonal polarizations in our experiment, we calculated the corresponding molecular alignment revival $<<cos^2\theta_\perp >>=(1-<<cos^2\theta_\parallel >>)/2$ along the filed polarization of the probe pulse as shown in Figs. 2(b) and 2(d), where $\theta_\perp$ is the angle between the molecular axis and the probe polarization. The refractive index seen by the probe pulse reads $\delta n_\perp = (2\pi\rho_0\Delta\alpha/n_0)(<<cos^2\theta_\perp >>-1/3)$, where ρ_0 is the initial molecular density, $\Delta\alpha=\alpha_\parallel-\alpha_\perp$ is the polarizability difference [22], n_0 is the linear refractive index. By considering the Gaussian-shaped transverse profile of the pump with more significant molecular alignment in the beam center than its periphery, the probe pulse experiences an additional cross-(de)focusing effect depending on the transient molecular orientation. The alignment-induced additional cross-(de)focusing competes the beam diffraction as $\delta n_\perp >(k_0Z_0)^{-1}$, where k_0 and Z_0 are respectively the wave-number and Rayleigh range of the probe beam [16]. For a pump intensity of 4.3×10^{13} W/cm^2 with $(<<cos^2\theta_\perp >>-1/3)\sim0.032$, the refractive index variation is estimated to be $\delta n_\perp \sim1.2\times10^{-5}$ for molecular O_2 with a polarizability difference of $\Delta\alpha=1.2$ Å^3 at a gas pressure of 2 atm. For a pump beam waist of ~50 μm, the beam diffraction of the probe pulse is estimated to be $(k_0Z_0)^{-1}\sim1.2\times10^{-5}\sim\delta n_\perp$, indicating an important role of the alignment-induced cross-(de)focusing effect in our experiments. Meanwhile, an additional time-dependent frequency shift due to the accumulated phase modulation from molecular

alignment revivals as $\delta\omega(t)\sim-\partial\delta n_\perp(t)/\partial t$ is introduced to the delayed probe pulse [19, 20]. The succeeding filamentation dynamics as well as the consequent SC generation is therefore dominated by the spatiotemporal phase modulation of the molecular alignment.
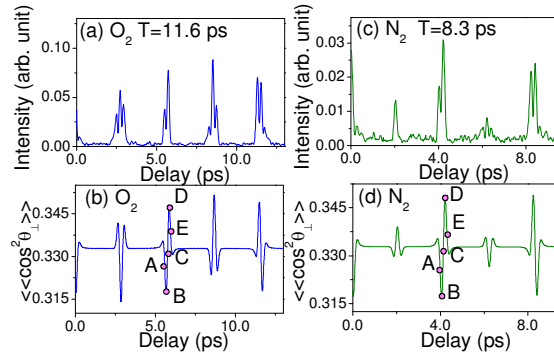

Fig. 2. (a) and (c) The measured molecular alignment signal of O_2 and N_2 by weak field polarization technique. (b) and (d) The calculated molecular alignment metric $<<cos^2\theta_\perp>>$ versus pump-probe delay.

Figure 3 shows the measured output spectra of the probe pulse as its temporal peak was tuned to various revival times [labeled in Fig. 2(b)] of the prealigned O_2 molecules with a pressure of 2 atm. As shown in Fig. 3(a), the spectrum of the probe pulse (dashed curve) was significantly broadened (from 525 to 900 nm) as compared with the input one (solid curve) when the molecules were randomly orientated (without pump). Here, the SPM, including contributions from time-dependent field intensity ($\sim\partial I/\partial t$) and electron density ($\sim\partial\rho/\partial t$) [23], plays an important role for the observed spectral broadening with a noticeable blue-shift, which is also closely related with the self-steepening and space-time focusing occurring in the filamentation process of the probe pulse. When the pump pulse was turned on, for instance at delay-A as shown in Fig. 3(b), the spectrum was slightly narrowed with weakened SPM process for the additional cross-defocusing effect from the perpendicularly orientated molecules with $(<<cos^2\theta_\perp>>-1/3)<0$. As shown in Fig. 3(c), the narrowest spectrum was observed around delay-B with most significant perpendicular molecular alignment. The output spectrum of the probe pulse was almost the same as the case of randomly orientated molecules when the temporal peak of the probe pulse was tuned to delay-C [Fig. 3(d)], where the molecular alignment degree, $<<cos^2\theta_\perp>>\sim1/3$, is close to the case without molecular alignment and hence lead to negligible cross-(de)focusing effect. However, as shown in Fig. 3(e) for delay-D, SC with noticeable extension in UV spectral region (cutoff at 370 nm) was observed for additional cross-focusing effect from the parallel molecular alignment revival, which hence enhanced the involved SPM. The final pulse energy of the generated SC was measured to be 1.2 mJ at the end of gas cell with a stable self-cleaned single core beam profile as shown in the inset of Fig. 1. The extension in the UV spectral region of the generated SC decreases rapidly as the probe pulse was tuned away from the optimal parallel revival of the molecular alignment shown in Fig. 3(f) for delay-E as example.

Both spatial and temporal phase modulations by molecular alignment revivals were introduced to the probe pulse to influence its succeeding filamentation dynamics [18] and SC generation. The SC generation with maximum UV extension around the maximum parallel molecular alignment revival indicated that the additional cross-focusing effect from spatial phase modulation played a more important role than the frequency modulation from temporal phase modulation, since the cross-focusing effect reached its maximum value for the maximum parallel revival (around delay-D) where the frequency modulation induced by the temporal phase modulation was close to zero [19, 20]. The frequency modulation proportional

to $|\partial\delta n_\perp(t)/\partial t|$ reached its maximum value around the transition time from parallel to perpendicular (or perpendicular to parallel) revivals with negligible spatial cross-(de)focusing effect, where almost no additional extension of SC generation was observed (delay-C) in our experiment. Therefore, the additional cross-focusing effect from the parallel revival of the molecular alignment enhanced SPM as well as self-steepening and space-time focusing effects to broaden the spectrum of the probe pulse, resulting in considerable UV extension of the generated SC observed in our experiments.
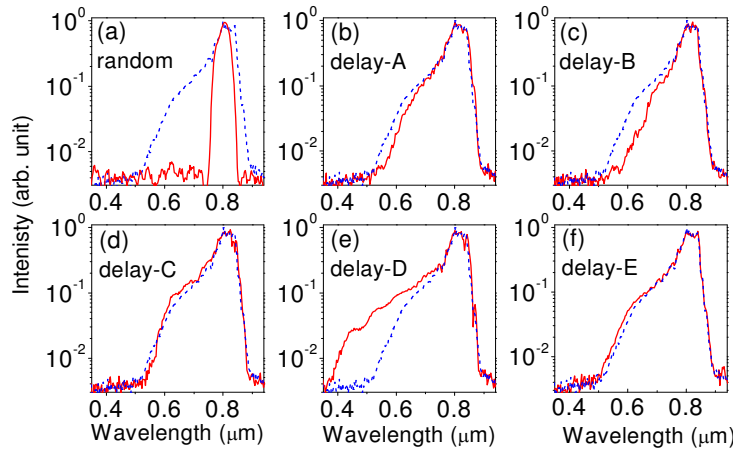

Fig. 3. The spectra of the probe pulse at the end of O_2 cell for (a) randomly orientated molecules (dashed curve) and (b)-(f) when it is tuned to various molecular alignment revivals as labeled in Fig. 2 (b). The dashed and solid curves stand for the output spectra of the probe pulse when the molecules are randomly orientated and prealigned, respectively. The solid curve in (a) is the input spectrum of the probe pulse.

The SC generation and extension by additional cross-focusing from the maximum parallel revival of molecular alignment (delay-D) was further proved by tuning the intensity of the pump pulse for molecular alignment as shown in Fig. 4(a), which directly changed the molecular alignment degree and hence the cross-focusing effect. The gas pressure of oxygen was set to be 2 atm. The extension of the spectrum in the UV region decreased gradually as the decreasing pump energy from 0.57 to 0.4 mJ, which corresponds to a variation of the pump intensity from 4.3×10^{13} to 3.0×10^{13} W/cm^2 around the geometric focus and molecular alignment degree $|<<cos^2\theta_\perp>>-1/3|$ from 0.032 to 0.022. Almost no additional spectral extension at short wavelengths was observed at pump intensities smaller than 2.6×10^{13} W/cm^2 for the negligible influence from molecular alignment.
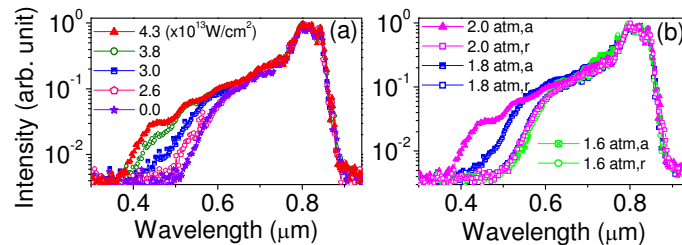

Fig. 4. (a) The evolution of the probe pulse spectra at the end of O_2 cell with different pump intensities for molecular alignment. (b) The UV extension of SC of the probe pulse in prealigned (labeled as a) and randomly orientated (labeled as r) O_2 molecules with different gas pressures.

Besides the degree of molecular alignment, the additional cross-focusing effect also closely depends on the number density of the involved molecules. As shown in Fig. 4(b), for parallel molecular alignment revival at delay-D, the extension of the generated SC at short

wavelengths decreased gradually as the gas pressure changed from 2.0 to 1.6 atm, with a fixed pump energy of 0.57 mJ and molecular alignment degree of $|<<cos^2\theta_\perp>>-1/3|\sim0.032$. However, when the molecular alignment was turned off without pump pulses, the output spectra of the probe pulses were almost unchanged for the decrease of the gas pressure from 2.0 to 1.6 atm, indicating a negligible influence of the variation of the material nonlinearities (estimated to be 20% by considering a linear dependence on the number density) on the spectral broadening of the probe pulse in our experiments. Obviously, molecular alignment with additional cross-focusing effect from parallel revival played a significant role for the observed SC extension at short wavelengths as a result of the consequently enhanced SPM and self-steepening effect during the succeeding filamentation.

For various diatomic molecules with different polarizability differences and nonlinearities, the influence of the molecular alignment revivals on the SC generation and extension is different. For example, in comparison with the above studied O_2 molecules with a polarizability difference of $\Delta\alpha=1.2$ Å^3 and nonlinear refractive index of $n_2=10.2\times10^{-19}$ cm^2/W at 2 atm, N_2 molecules shows a polarizability difference of $\Delta\alpha=1.0$ Å^3 and nonlinear refractive index of $n_2=4.6\times10^{-19}$ cm^2/W at 2 atm [24, 25]. The smaller polarizability difference of N_2 [Fig. 2(c)] as compared with O_2 [Fig. 2(a)] could be seen clearly from the relative magnitudes of the measured molecular alignment signals for the same experimental conditions. Therefore, aligned N_2 molecules are expected to produce weaker effects on the extension of the generated SC than prealigned O_2 molecules. Figure 5 shows the spectral evolution of the probe pulse when its temporal peak was tuned to various revivals of the molecular alignment of N_2 [labeled as A-E in Fig. 2(d)]. Similar to O_2 molecules as shown in Fig. 3, the output spectra of the probe pulse were narrowed for the perpendicular molecular alignment revival of N_2 molecules [Figs. 5(b) and 5(c)], and SC generations with noticeable extension in the UV region was observed for the parallel molecular alignment revival [Fig. 5(e)]. However, the UV extension of the generated SC for the maximum parallel revival around delay-D with aligned N_2 molecules was not as much as that of the aligned O_2 molecules, which was originated from the relative smaller polarizability difference ($\Delta\alpha$) of N_2.
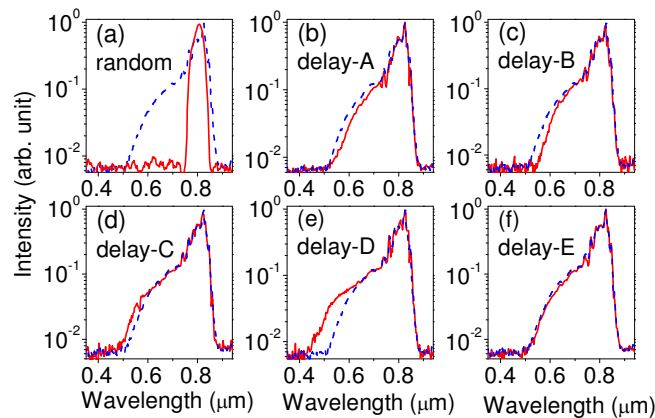

Fig. 5. The spectra of the probe pulse at the end of N_2 cell with same presentation as Fig. 3.

The relatively weaker influence of aligned N_2 molecules on the SC generation and extension in the UV spectral region were also confirmed by tuning the pump intensity and gas pressure around the maximum parallel revival, which are shown in Fig. 6. The changes of the output spectra versus the gas pressure and pump intensity were similar for both O_2 and N_2 molecules as considered, while the variation of the spectral range was smaller for N_2 (Fig. 6) than O_2 (Fig. 4). For N_2 molecules at 2 atm, as shown in Fig. 6(a), the spectral UV extension was vanished when the pump intensity is around 0.6×10^{13} W/cm^2, which is estimated to be 2.6×10^{13} W/cm^2 for molecular O_2. It indicates a more closer dependence of SC generation and extension on the alignment degree of O_2, which was consistent with its larger value of

polarizability difference. For the relative small nonlinear refractive index of N_2 molecules, as shown in Fig. 6(b), the spectra of the probe pulse narrowed gradually as the decreasing of the gas pressure for the both cases with and without molecular alignment, which differed from O_2 molecules as shown in Fig. 4 (b).
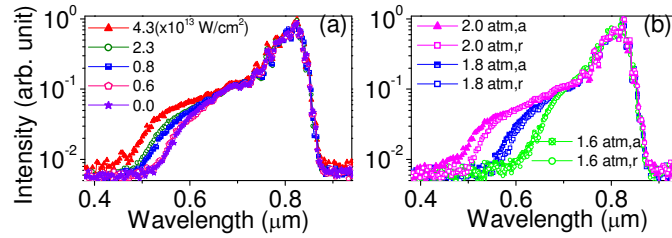

Fig. 6. (a) The evolution of the probe pulse spectra at the end of N_2 cell with different pump intensities for molecular alignment. (b) The UV extension of SC of the probe pulse in prealigned (labeled as a) and randomly orientated (labeled as r) N_2 molecules with different gas pressures.

4. Conclusion

In summary, we have studied the UV extension of SC generation by filaments in prealigned diatomic molecules of O_2 and N_2 with various pump intensities, gas pressures and molecular alignment revivals. The experimental results showed that the additional cross-focusing effects resulted from the spatial modulation of the refractive index by the parallel aligned molecules dominated the UV extension of SC, which closely depended on the polarizability difference ($\Delta\alpha$) and nonlinear refractive index (n_2) of the involved molecules. It therefore could be used as a flexible method to manipulate the UV extension of SC generation in molecular gases.

Acknowledgments